

Quantitative Upper Airway Imaging with Anatomic Optical Coherence Tomography

Julian J. Armstrong, Matthew S. Leigh, David D. Sampson, Jennifer H. Walsh, David R. Hillman, and Peter R. Eastwood

Optical+Biomedical Engineering Laboratory, School of Electrical, Electronic, and Computer Engineering, and School of Anatomy and Human Biology, University of Western Australia, Crawley; and West Australian Sleep Disorders Research Institute, Department of Pulmonary Physiology, Sir Charles Gairdner Hospital, Nedlands, Western Australia, Australia

Background: Measurements of upper airway size and shape are important in investigating the pathophysiology of obstructive sleep apnea (OSA) and in devising, applying, and determining the effectiveness of treatment modalities. We describe an endoscopic optical technique (anatomic optical coherence tomography, *aOCT*) that provides quantitative real-time imaging of the internal anatomy of the human upper airway.

Methods: Validation studies were performed by comparing *aOCT*- and computed tomography (CT)-derived measurements of cross-sectional area (CSA) in (1) conduits in a wax phantom and (2) the velo-, oro-, and hypopharynx during wakefulness in five volunteers. *aOCT* scanning was performed during sleep in one subject with OSA.

Results: *aOCT* generated images of pharyngeal shape and measurements of CSA and internal dimensions that were comparable to radiographic CT images. The mean difference between *aOCT*- and CT-derived measurements of CSA in (1) the wax phantom was 2.1 mm² with limits of agreement (2 SD) from -13.2 to 17.4 mm² and intraclass correlation coefficient of 0.99 ($p < 0.001$) and (2) the pharyngeal airway was 14.1 mm² with limits of agreement from -43.7 to 57.8 mm² and intraclass correlation coefficient of 0.89 ($p < 0.001$). *aOCT* generated quantitative images of changes in upper airway size and shape before, during, and after an apneic event in an individual with OSA.

Conclusions: *aOCT* generates quantitative, real-time measurements of upper airway size and shape with minimal invasiveness, allowing study over lengthy periods during both sleep and wakefulness. These features should make it useful for study of upper airway behavior to investigate OSA pathophysiology and aid clinical management.

Keywords: optical coherence tomography; sleep apnea; upper airway anatomy

Measurements of upper airway size and shape are important in investigating the pathophysiology of obstructive sleep apnea (OSA) and in devising, applying, and determining the effective-

ness of treatment modalities (1). However, a persisting limitation is the absence of an imaging technique that satisfactorily provides safe, accurate, and repetitive measurements of upper airway dimensions during wakefulness and sleep. Radiographic computed tomography (CT) and fluoroscopy involve potentially hazardous ionizing radiation. Magnetic resonance imaging (MRI) is expensive, noisy, claustrophobic, and incompatible with metallic probes and catheters. Neither modality is suitable for lengthy evaluations or evaluations during sleep (2). Ultrasound is not feasible because of poor transducer-air coupling, an unavoidable problem in air-filled organs. Fiber-optic nasoendoscopy has been used to visually examine the anatomic features and structure of the airway, but its quantification of airway dimensions is indirect and subjective (3). Measurement of airway caliber using acoustic reflection is not possible distal to the site of collapse, because the acoustic waves will not penetrate a collapsed airway (4).

In this article, we describe an endoscopic optical technique that generates quantitative, real-time images of the upper airway that enable accurate determination of shape and size. Briefly, an optical probe is placed inside a catheter, which is inserted via the nares to the level of the midesophagus. Rotation of the probe within the catheter provides a 360° profile of surrounding tissue. The optical probe can be systematically moved within the catheter, allowing the upper airway to be scanned at multiple sites without stimulating the airway mucosa.

The technique is adapted from optical coherence tomography (OCT) (5), a medical imaging modality. OCT is an optical sectioning microscopy modality that has been used to image subsurface tissue morphology in fields including ophthalmology (6), dermatology (7), vascular medicine (8), gastroenterology (9), and urology (10). Our adaptation involves a substantial increase in its axial distance range to allow macroscopic imaging of upper airway internal anatomy. We refer to this adaptation as “anatomic OCT” (*aOCT*) to distinguish it from the existing microscopic, subsurface OCT techniques (11).

This article presents the operational capabilities of the system, including data regarding its validity and applicability to quantitative measurement of human upper airway size and shape.

METHODS

Baseline *in vitro* validation studies were performed by comparing *aOCT*-derived measurements of cross-sectional area (CSA) with those derived from (1) circular holes of known size in a wooden template and (2) CT-derived measurements of holes with varying shape and size cut in a wax phantom. After these measurements, *in vivo* studies were performed to (1) compare *aOCT*-derived measurements of upper airway shape and size at the levels of the velo-, oro-, and hypopharynx with those obtained from simultaneous CT scans and (2) determine the reproducibility, and intra- and interobserver variability of *aOCT*-derived measurements of upper airway shape and size. Additional *in vivo* measurements were performed to demonstrate the feasibility of undertaking such measurements to determine pharyngeal compliance and, in one patient with OSA, during sleep.

(Received in original form July 26, 2005; accepted in final form October 14, 2005)

Supported by the Medical Research Foundation of Western Australia and the Australian Health Management Group and by the National Health and Medical Research Council (Australia; development grant no. 303319). These funding contributors had no role in study design, data collection, data analysis, data interpretation, or writing of the report. PRE is supported by a National Health and Medical Research Council (Australia) R. Douglas Wright Fellowship (no. 294404).

Correspondence and requests for reprints should be addressed to Julian Armstrong, B.Sc., B.E. (Hons), Optical+Biomedical Engineering Laboratory, School of Electrical, Electronic, and Computer Engineering, University of Western Australia, 35 Stirling Highway, Crawley, Western Australia 6009. E-mail: julian-a@ee.uwa.edu.au

This article has an online supplement, which is accessible from this issue's table of contents at www.atsjournals.org

Am J Respir Crit Care Med Vol 173, pp 226–233, 2006
Originally Published in Press as DOI: 10.1164/rccm.200507-1148OC on October 20, 2005
Internet address: www.atsjournals.org

Approvals for all measurements in human volunteers were obtained from the Human Research Ethics Committees of Sir Charles Gairdner Hospital and the University of Western Australia. Informed consent was obtained from all subjects.

Description of *a*OCT

In this technique (12), an optical probe is placed inside a sealed, transparent catheter (3.0 mm outer diameter) that is inserted via the nares to the level of the midesophagus. In awake subjects, the minor discomfort associated with the insertion of the catheter is minimized by application of topical anesthetic (10% lidocaine spray) to the mucosa of the upper airway (throat and nose). Once in position, the catheter is taped to the external nares. The probe can be systematically moved within the catheter without displacing it and therefore without stimulating the airway mucosa. A minimum of 20 min is allowed for the effects of the lidocaine to remit before measurements are obtained.

The system operates by directing a light beam perpendicular to the catheter. The distance between the probe head and the air–tissue interface of the airway wall is determined from the reflected light using a low-coherence optical interferometer. The probe rotates at 1.25 Hz to capture quantitative cross-sectional images of the upper airway lumen, in much the same way that a radar system captures an image. A customized computer program controls a motorized translation stage that allows the probe head to be precisely rotated and precisely translated to various levels within the pharynx to record cross-sections of interest. These tomograms can be viewed graphically in real time on a personal computer or reconstructed in the form of a video. Additional details regarding the technique can be found in the online supplement.

Validation Studies

In vitro bench studies. The accuracy of the technique was assessed *in vitro* in two ways. First, the *a*OCT system was used to measure the CSA of circular holes of known size in a template constructed from wood. An *a*OCT scan was obtained with the probe fixed inside each hole, and the resulting images were thresholded to distinguish the interior region, then pixels counted (Matlab; Mathworks, Natick, MA) to determine the CSA. Second, a phantom target was imaged simultaneously with *a*OCT and CT (third-generation CT scanner, HiSpeed CTi [GE Healthcare, Chalfont St. Giles, United Kingdom], with voltage and tube current set to optimize CT image quality, 80 kV, 100 mA). The phantom consisted of a paraffin wax block into which multiple holes were cut of varying shape and size. Wax was used as a material because it is readily shaped and because for CT it has similar properties to human tissue. *a*OCT and CT cross-sectional images were obtained at the same location and orientation for each hole.

In vivo validation studies. The system was then assessed *in vivo*. All *in vivo* studies were commenced with a “pullback” scan. This was achieved by systematically retracting the optical probe at a constant speed (0.2 mm/s⁻¹) from the upper esophagus to the nasal cavity while the subject was breathing quietly. Each resulting dataset was used to construct a movie of the pullback scan, thereby allowing convenient mapping of pharyngeal dimensions and anatomical landmarks, including specific sites for further investigation. For the studies described in the following section, the optical probe was then moved to the relevant level in the airway to obtain detailed cross-sectional information for analysis.

***a*OCT versus CT.** Simultaneous *a*OCT and CT images of the upper airway were obtained in five healthy subjects without OSA (one male and four females; mean age, 27 yr; body mass index, 22.3). Subjects were awake, supine, breathing quietly with the head maintained in a neutral position using a Shea headrest (Gyrus ENT, Memphis, TN). At the end of a normal exhalation (i.e., at functional residual capacity), each subject momentarily held his or her breath while simultaneous scans were obtained. The CT scanner was adjusted to scan through the tip of the probe orthogonal to the airway so that the *a*OCT and CT scan planes were coincident. Scans were obtained at the level of (1) the hypopharynx, 20 mm caudad to the tip of the epiglottis; (2) the oropharynx, just cranial to the tip of the epiglottis; and (3) the velopharynx (retropalatal pharynx), just cranial to the palatal rim.

Reproducibility and intra- and interobserver variability. The reproducibility of *a*OCT-derived measurements of pharyngeal dimensions was assessed by scanning five healthy subjects without OSA (one male

and four females; mean age, 27 yr; body mass index, 22.3) on two separate occasions (separated by ≥ 24 h). On each occasion, dimensions were calculated from *a*OCT images obtained at the same level at each of three identical locations (velo-, oro-, and hypopharynx) within the upper airway.

To assess intra- and interobserver variability of *a*OCT-derived measurements of pharyngeal dimensions, 10 images of each of the velo-, oro-, and hypopharynx were randomly selected from a database containing images from 10 subjects and analyzed by two observers on two separate occasions (separated by ≥ 24 h).

Feasibility Studies

Measurement of pharyngeal compliance. The feasibility of measuring pharyngeal compliance during wakefulness using *a*OCT technique was investigated in 10 subjects with OSA and 8 nonsnoring control subjects (see Table E1 in the online supplement). Each individual was fitted with a nasal mask via which variable levels of continuous positive airway pressure could be applied. *a*OCT scans were performed and CSA at the velo-, oro-, and hypopharynx measured while continuous positive airway pressure was maintained for 2 min at each of 3, 6, 9, 12, and 15 cm H₂O. At each scanning level, CSA was plotted against applied mask pressure. The slope of this relationship (regression analyses) was defined as pharyngeal compliance. Separate area–pressure relationships were plotted for the minimum and maximum airway dimensions at each level.

***a*OCT scanning during sleep.** The feasibility of monitoring upper airway shape and size changes during sleep using *a*OCT was investigated in one male subject with severe OSA (apnea–hypopnea index, 51; age, 69 yr; body mass index, 25.9). This individual was instrumented for full overnight polysomnography (13) and *a*OCT scanning.

Analyses

Analyses of *a*OCT images were performed using ImageJ software (National Institutes of Health, Bethesda, MD). The mucosa–lumen interface was manually traced and airway CSA calculated. Anteroposterior diameter was calculated in the midsagittal plane and lateral diameter was measured at the widest point in the coronal plane, perpendicular to the anteroposterior diameter.

Regression analyses were performed with the least-squares method. Measurements of pharyngeal compliance were compared between groups at each site using two-way repeated measures analysis of variance. A Holm-Sidak test was applied for all post-hoc comparisons. The Bland-Altman test (14) and the intraclass correlation coefficient (15) were used to evaluate the agreement between *a*OCT and CT-derived measurements of CSA from the wax phantom and pharyngeal dimensions, and to evaluate reproducibility and intra- and interobserver variability of *a*OCT-derived measurements.

RESULTS

Validation Studies

In vitro bench studies. The percentage errors in *a*OCT-derived measurements of CSA for five holes drilled in a template constructed from wood with radii of 5, 10, 15, 20, and 25 mm were 0.3, 0.6, 0.3, -2.7, and -1.1%, respectively. The mean error was -0.5%, or 0.1 cm², which corresponded to a mean error in radius of 0.07 mm.

The differences in CSA of 23 conduits of varying shape and size cut in a wax phantom are demonstrated in a Bland-Altman plot (Figure 1). The average CSA obtained using *a*OCT and CT was 610 \pm 500 and 608 \pm 499 mm², respectively. The mean difference between the measurements of CSA obtained with the two techniques was 2.1 mm² with limits of agreement (2 SD) from -13.2 to 17.4 mm² and an intraclass correlation coefficient of 0.99 ($p < 0.001$). The mean differences between measurements of anteroposterior and lateral diameters were small, being 0.31 and 0.54 mm, respectively. The intraclass correlation coefficient was 0.99 for measurements of anteroposterior ($p < 0.001$) and lateral diameters ($p < 0.001$).

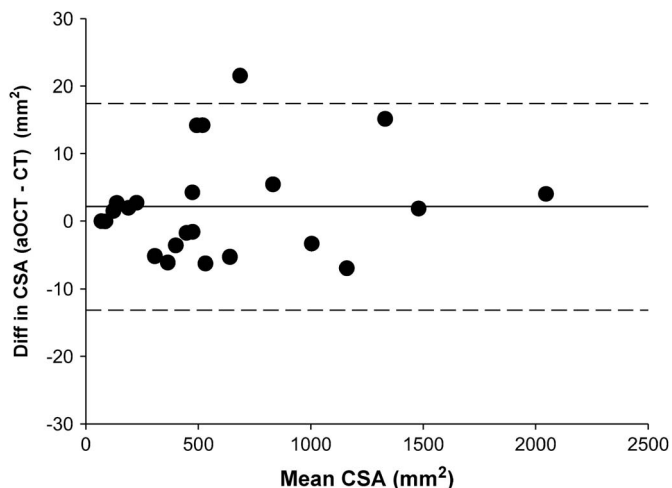


Figure 1. Bland-Altman plot of the agreement between measurements of cross-sectional area (CSA) derived from anatomic optical coherence tomography (aOCT) and computed tomography (CT) scans in 23 conduits of varying size and shape cut in a wax phantom. The solid line represents the mean difference between the two methods (systematic bias), and the dashed lines define the limits of agreement (± 2 SD).

In Vivo Validation Studies

Pullback scans. Figure 2 shows lateral and anteroposterior longitudinal reconstructions from a pullback scan with six cross-sectional images at locations spaced at intervals along the pharynx. A movie created from the pullback scan (see Video E1) is available in the online supplement. A number of anatomic features are indicated on the images. The dark lines in the images are the air-tissue boundaries of the lumen; for the cross-sections these are traced out by the aOCT system during a single rotation. The tissue-air boundaries in the figure appear fuzzy, because aOCT also detects subsurface reflections, but the air-airway wall interface is sharp, allowing accurate surface location.

aOCT versus CT. Figure 3 shows representative examples of simultaneous aOCT and CT scans at each of the three levels in one healthy subject without OSA. A Bland-Altman plot of the pooled difference in CSA using the two techniques in five healthy subjects is shown in Figure 4. The average CSA obtained using aOCT and CT was 133.2 ± 61.4 and 147.4 ± 59.7 mm², respectively. The mean difference between measurements obtained with the two techniques was 14.1 mm² with limits of agreement (2SD) from -43.7 to 57.8 mm². The mean difference in measures of anteroposterior and lateral diameters was 0.7 and 0.4 mm, respectively, with limits of agreement from -3.5 to 4.8 mm and -6.8 to 7.6 mm, respectively. The intraclass correlation coefficients for measurements of CSA and anteroposterior and lateral diameters were 0.89, 0.66, and 0.82, respectively ($p < 0.05$ for all). Data for measurements obtained at each of the three sites are shown in Table 1 and Tables E2 and E3.

Reproducibility. To assess reproducibility, five individuals were scanned with aOCT on two separate occasions, and measurements of pharyngeal dimensions obtained at the same locations within the velo-, oro-, and hypopharynx using the same observer to derive the measurements. The average CSA on the first testing occasion was 161.2 ± 43.6 , 226.9 ± 42.8 , and 210.3 ± 91.4 mm², respectively, and 167.9 ± 60.8 , 242.6 ± 45.7 , and 188.1 ± 93.3 mm² on the second occasion. The mean difference between the two testing days was 6.7, 15.7, and 22.2 mm², respectively, and the intraclass correlation coefficients for measure-

ments obtained on the two testing days were 0.75, 0.70, and 0.97, respectively ($p < 0.01$ for all; Table 1). The mean difference and intraclass correlation coefficients between duplicate measurements of anteroposterior and lateral diameters are reported in Tables E2 and E3.

Intraobserver variability. To assess intraobserver variability, 10 aOCT images were randomly selected for measurement of pharyngeal dimensions at the level of the velo-, oro-, and hypopharynx on two separate occasions by each of two observers. The average CSA on the first measurement occasion was 180.3 ± 121.5 , 284.1 ± 167.8 , and 452.4 ± 135.3 mm², respectively, and 178.8 ± 120.5 , 281.4 ± 167.4 , and 451.8 ± 131.7 mm² on the second occasion. The mean difference (pooled data) between these duplicate measurements was small, being 1.4, 2.7, and 0.6 mm², respectively, and the intraclass correlation coefficients were 0.99 for all ($p < 0.001$ for all; Table 1). The mean differences and intraclass correlation coefficients between duplicate measurements of anteroposterior and lateral diameters were also small (see Tables E2 and E3).

Interobserver variability. To assess interobserver variability, the results of the analyses of the images by the two observers were compared. The average CSA at the velo-, oro-, and hypopharynx was 180.9 ± 120.9 , 281.4 ± 166.2 , and 450.2 ± 131.4 mm², respectively, from Observer 1, and 179.2 ± 121.2 , 284.0 ± 169.0 , and 454.0 ± 135.6 mm² from Observer 2. The mean difference between the two observers was 0.7, 2.6, and 3.9 mm², respectively, and the intraclass correlation coefficients were 0.99 for all ($p < 0.001$ for all; Table 1). The mean differences between the observers for measurements of anteroposterior and lateral diameters were also small (see Tables E2 and E3).

Feasibility Studies

Measurement of pharyngeal compliance. The slope of the relationship describing change in upper airway size with increasing airway pressure defined pharyngeal compliance (Figure 5). CSA varied with phase of respiration. Using maximal CSA, measures of compliance at the velo-, oro-, and hypopharynx were 5.8 ± 1.9 , 7.1 ± 1.8 , and 9.7 ± 1.9 mm²/cm H₂O for control subjects and 2.3 ± 1.6 , 7.5 ± 1.6 , and 12.3 ± 1.6 mm²/cm H₂O for individuals with OSA ($p < 0.05$ for velopharynx vs. hypopharynx, oropharynx vs. hypopharynx, and velopharynx vs. oropharynx in the OSA group only). Using minimal CSA, measures of compliance at the velo-, oro-, and hypopharynx were 4.1 ± 2.0 , 5.8 ± 1.8 , and 8.1 ± 2.0 mm²/cm H₂O for control subjects and 2.2 ± 1.6 , 6.4 ± 1.6 , and 12.1 ± 1.6 mm²/cm H₂O for individuals with OSA ($p < 0.05$, velopharynx vs. hypopharynx and oropharynx vs. hypopharynx in the OSA group only). A movie (see Video E2) of a representative pharyngeal compliance study for one subject is available in the online supplement.

aOCT scanning during sleep. Figure 6 demonstrates changes in upper airway size and shape before, during, and after airway collapse (i.e., an apneic event) in an individual with OSA. Images were collected in the velopharynx while the subject was in stable stage 2 sleep. The 10 selected aOCT cross-sectional images in Figures 6a–6j show the airway changing size during normal unobstructed breathing, being smaller during inspiration than expiration (a–d); the airway narrowing (e) then collapsing during a 5-s apnea (f); collapsing during a 12-s apnea (g, h); and restoration of an open airway after momentary arousal from sleep (i, j). Video E3 shows aOCT data of the apneic event.

DISCUSSION

This study reports on a new optical technique that can provide quantitative real-time imaging of the internal anatomy of the human upper airway. The impetus for this work has been the

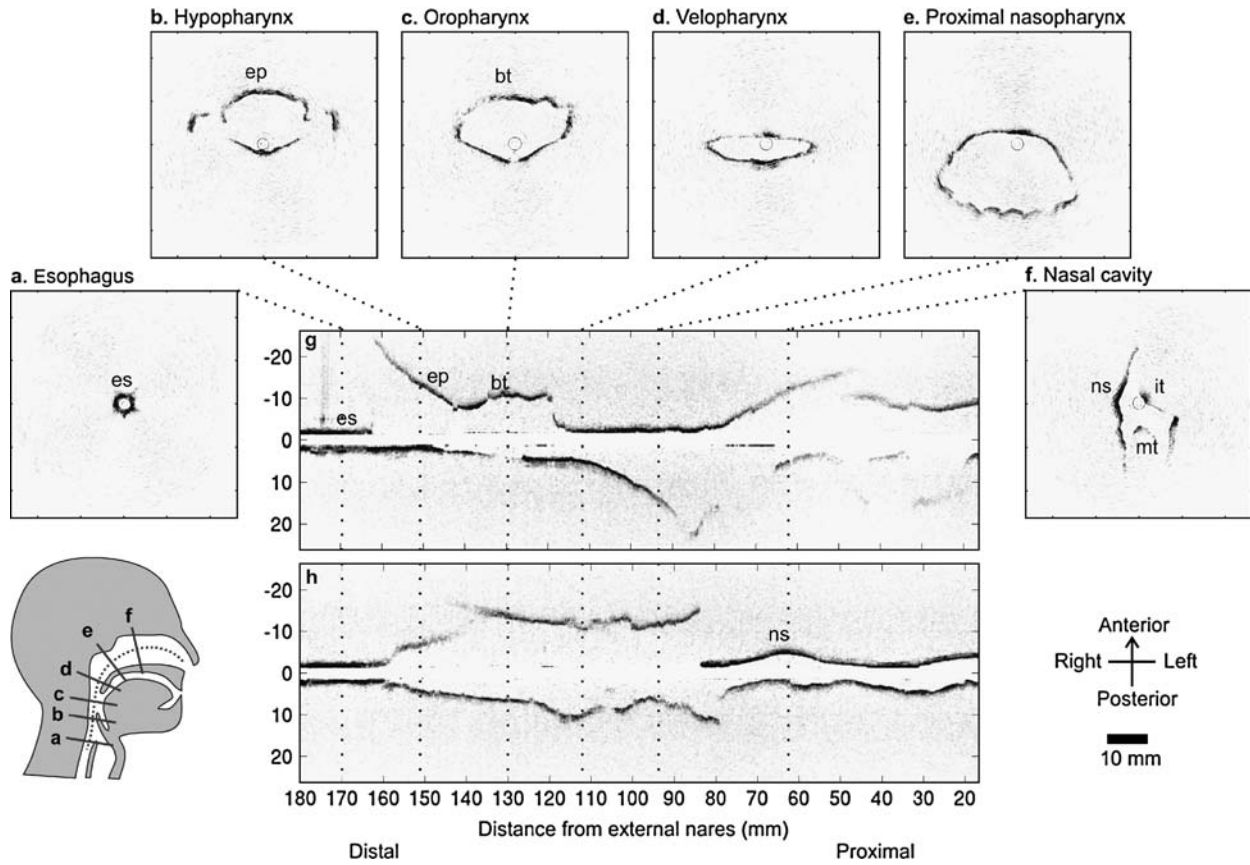


Figure 2. Selected images from a “pullback scan” of a subject without sleep apnea. The 163-mm scan started in the upper esophagus (180 mm from the external nares). (a–f) Images of 52 × 52-mm cross-sections selected to show various anatomic features of the pharynx and nasal cavity. (g, h) Anteroposterior (g) and lateral (h) sections relative to the catheter. bt = base of tongue; ep = epiglottis; es = esophagus; it = inferior turbinate; mt = middle turbinate; ns = nasal septum.

long-recognized need to quantitatively evaluate changes in human upper airway size and shape during sleep. Such measurements are of particular value in understanding the pathophysiology of OSA and in devising, applying, and determining the effectiveness of treatment modalities (1).

In recent years, upper airway size and shape have been measured by a number of techniques, including CT (16–18), fluoroscopy (19, 20), MRI (21–24), nasoendoscopy (25–28), and acoustic reflection (4, 29, 30). Although these studies have demonstrated important differences in pharyngeal shape and size between

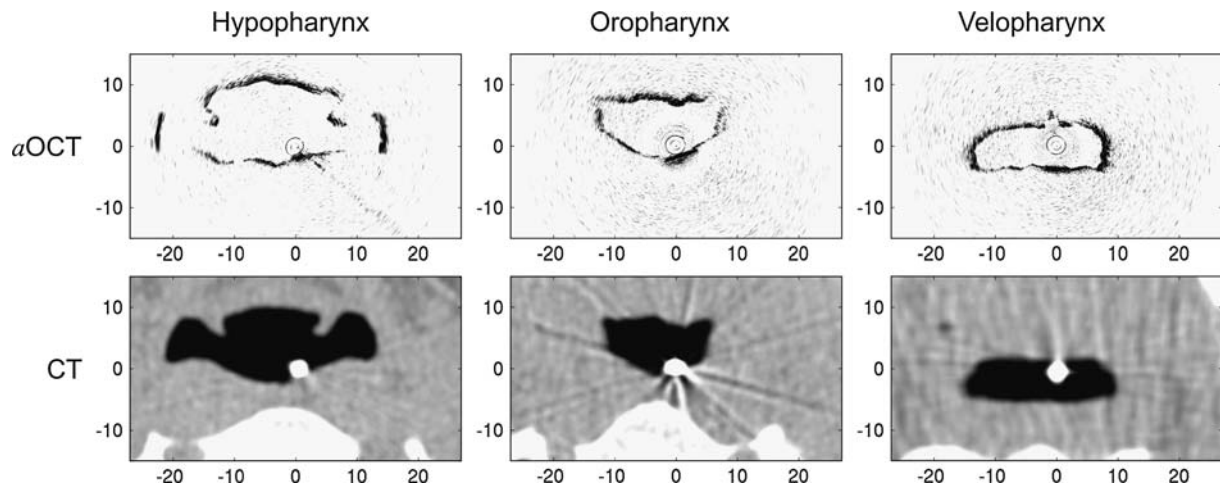


Figure 3. Simultaneous *a*OCT scans and CT scans obtained in the hypopharynx, oropharynx, and velopharynx. All images are shown on the same scale, with numbers indicating distance in millimeters.

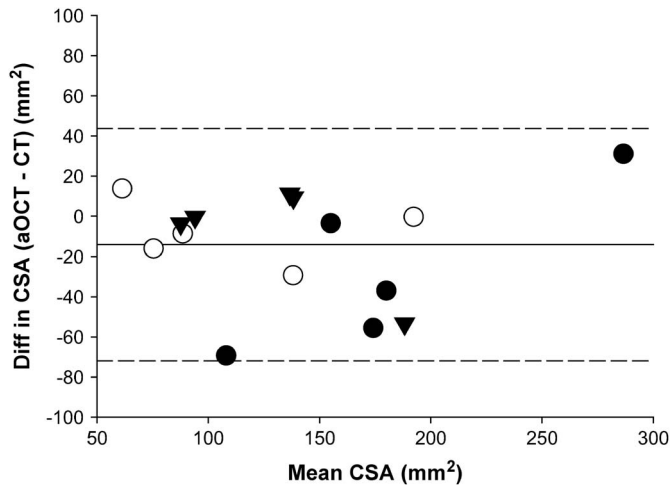


Figure 4. Bland-Altman plots of the agreement between measurements of CSA derived from simultaneous *aOCT* and CT scans in the hypopharynx (closed circles), oropharynx (open circles), and velopharynx (closed triangles) in five healthy subjects without sleep apnea. The solid line represents the mean difference between the two methods (systematic bias); the dashed lines define the limits of agreement (± 2 SD).

individuals with and without OSA, in terms of baseline anatomy (4, 16, 18, 22, 23, 29, 30) and dynamic behavior (17, 19–21, 24–28), the routine use of these technologies for study of the upper airway on repeated occasions and over prolonged periods in individuals is limited. We present *aOCT* as a useful addition to these existing technologies. Its minimal invasiveness, quietness, comfort, and lack of potentially hazardous effects (such as ionizing radiation) make it suitable for study of pharyngeal size and shape over prolonged periods during both sleep and wakefulness.

The *in vitro* measurements illustrate the precision of the method in obtaining measurements of shape and size. The differences between *aOCT* and CT-derived measures of anteroposterior and lateral dimensions were very small (0.4 mm on average), and the high intraclass correlation coefficients demonstrate that the two techniques provide comparable measurements. CSA measurements tended to be slightly larger when measured using *aOCT* (by 2.1 mm² on average), although the high intraclass

correlation coefficients demonstrate that the two techniques show good agreement.

In each of the *in vivo* studies presented in this article, *aOCT* scanning was commenced with a pullback scan (Figure 2). This was achieved by systematically retracting the optical probe from the upper esophagus to the nasal cavity while the subject was breathing quietly. There is no sensation of movement of the probe because it is retracted within a fixed catheter, thereby avoiding stimulation of the airway mucosa. Also, because the mass of the rotating fiber probe is exceedingly low and substantially less than the plastic catheter, significant mechanical vibration does not transfer from the probe to the catheter. The benefit of this was demonstrated in the one subject who was studied during sleep (see Figure 6), where the probe was moved to various sites in the upper airway without causing arousal.

On completion of the pullback scan, each resulting data set was then used to construct a movie (see Video E1). Although the movie constitutes a useful dataset in its own right, it can also be used to identify specific sites for further investigation. In such circumstances, the optical probe is moved to those sites and continuous scanning undertaken to monitor the upper airway during steady-state conditions, state changes (e.g., changes in sleep stage or posture), or imposed changes (e.g., changes in airway pressure).

aOCT generated images of pharyngeal cross-sections that were comparable to images obtained by radiographic CT. The differences between *aOCT*- and CT-derived measures of anteroposterior and lateral dimensions were small (0.8 mm on average) at all levels. CSA measurements tended to be smaller with *aOCT*, particularly at the level of the hypopharynx. The most likely contributors to this difference were the misalignment between the *aOCT* and CT scan planes (caused by restricted movement of the CT gantry or occasional head/neck movement between the time of the CT scout scan and the cross-sectional scan), and obscuration of small parts of the airway wall during *aOCT* scanning (particularly at the hypopharynx; Figure 3). This obscuration, which is a limitation of the *aOCT* technique (see **METHODOLOGIC CONSIDERATIONS**), may also have contributed to the larger difference in CSA of the hypopharynx relative to other levels when individuals were measured on two separate occasions. Other contributors to this variability include position of the tongue and soft palate and differences in head and neck position, although the latter were minimized as far as possible between the two testing occasions.

TABLE 1. BLAND-ALTMAN ANALYSIS OF DIFFERENCES IN ANATOMIC OPTICAL COHERENCE TOMOGRAPHY-DERIVED MEASUREMENTS OF AIRWAY CROSS-SECTIONAL AREA

	No. Subjects	No. Measurements	Region	Intraclass			Limits of Agreement (-2 SD, 2 SD)
				Correlation Coefficient	Mean Difference (Bias)	95% CI	
CT vs. <i>aOCT</i>	5	5	VP	0.81	8.12	20.16	-24.35, 40.59
	5	5	OP	0.96	7.42	32.85	-45.49, 60.33
	5	5	HP	0.82	26.86	50.57	-54.60, 108.32
Reproducibility (Test 1 vs. 2)	5	15	VP	0.75	-6.7	20.73	-81.6, 68.2
	5	13	OP	0.70	-15.7	20.85	-84.7, 53.3
	5	12	HP	0.97	22.2	14.71	-24.1, 68.5
Intraobserver variability, <i>aOCT</i> (Observation 1 vs. 2)	10	20	VP	0.99	-1.43	2.21	-10.86, 8.00
	10	20	OP	0.99	-2.69	3.54	-17.83, 12.44
	10	20	HP	0.99	-0.56	5.50	-24.07, 22.95
Interobserver variability, <i>aOCT</i> (Observer 1 vs. 2)	10	20	VP	0.99	-0.73	2.66	-12.10, 10.63
	10	20	OP	0.99	2.61	3.71	-13.24, 18.46
	10	20	HP	0.99	3.89	5.88	-21.25, 29.02

Definition of abbreviations: *aOCT* = anatomic optical coherence tomography; CI = confidence interval; HP = hypopharynx; OP = oropharynx; VP = velopharynx. Data for mean difference, 95% CI, and limits of agreement are in square millimeters.

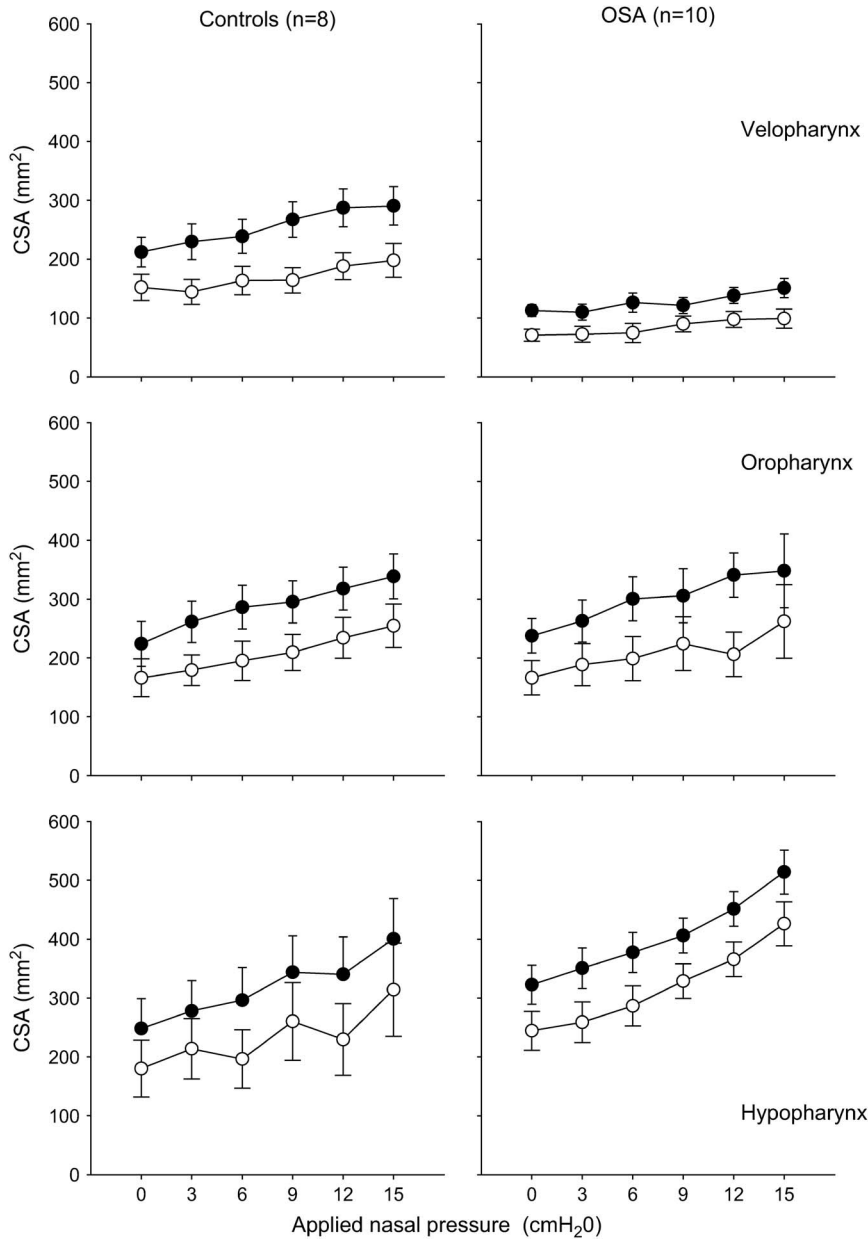


Figure 5. The effect of changing airway pressure on maximum (*closed circles*) and minimum (*open circles*) CSA at the level of the velo-, oro-, and hypopharynx. Measurements were obtained during wakefulness in subjects without (five female, three male) and with (four female, six male) obstructive sleep apnea (OSA); mean data \pm SE. Subjects were not matched for age, sex, or body mass index; thus, comparison of CSA between groups is not meaningful.

Methodologic Considerations

Measurement of upper airway anatomy using *a*OCT requires insertion of a catheter of similar dimensions to a nasogastric tube, within which the probe is housed. It is possible that the presence of the catheter may alter airway behavior, disturb sleep, and alter sleep architecture. Although our study did not specifically address this issue, previous investigations have shown that overnight catheter-based measurements of esophageal pressure, the current reference standard for measuring respiratory effort (31), (1) is acceptable in the majority of patients (96%) with catheter discomfort and insertion difficulty being extremely uncommon (32), (2) has no significant effect on sleep quality or on respiratory events (33), and (3) has minimal effect on sleep architecture (34). The size of the catheter in those studies was approximately 1.9 mm in diameter. It is probable that the larger the catheter the greater the potential for sleep disturbance. This was likely to be the case in the study by Hessel and colleagues (35) who, when using a catheter of 4.0 mm diameter, reported

that only half of their patients completed a whole night with the tube in place. The diameter of the current *a*OCT catheter is 3.0 mm. The optics system we currently use has an outer diameter of 1.3 mm. It is feasible to house the system in a narrower plastic catheter of 1.5 mm internal diameter and 2.0 mm outer diameter.

*a*OCT has the capacity to continuously measure changes in airway dimensions under a variety of conditions. Such changes can be seen during tidal breathing in each of the supplementary videos, and before, during, and after an apneic event in an individual with OSA (Figure 6). The images obtained from this individual show the potential of the technique to describe the patterns of change in airway shape and size that lead up to upper airway collapse. In this individual, the upper airway narrowed and then closed during expiration (e.g., frames *e* and *f*), consistent with previous analyses of airflow data (36), nasoendoscopy images (37), and CT images (38).

When CSA is related to changes in airway pressure, a measure of pharyngeal compliance can be derived as shown in Figure 5.

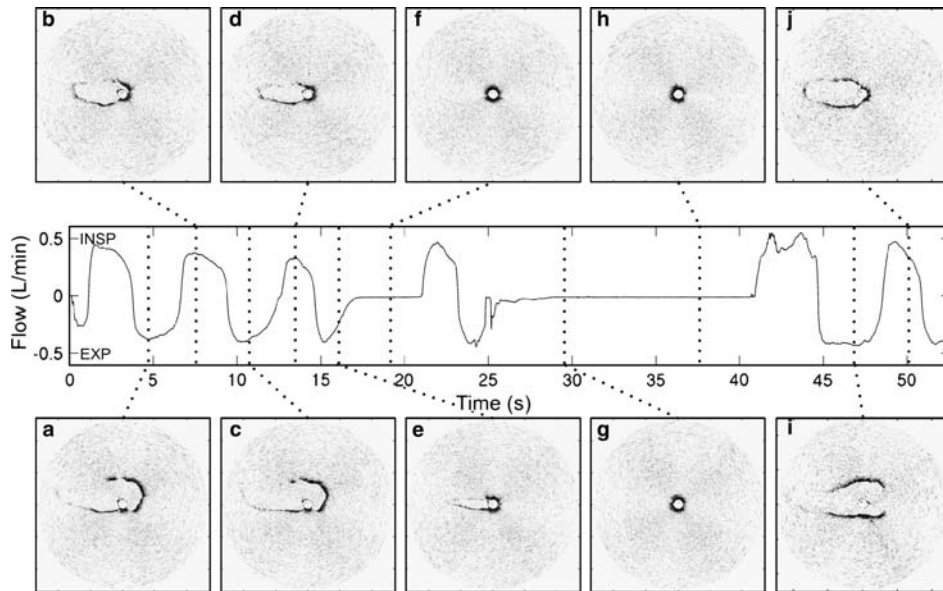


Figure 6. Changes in upper airway caliber before, during, and after airway collapse (i.e., an apneic event) in an individual with obstructive sleep apnea. The 5- and 12-s apneic events are clearly observed in both the respired airflow recording (*center plot*) and the series of airway images (*a-j*). INSP and EXP refer, respectively, to inspiration and expiration.

The finding that, in individuals with OSA, the pharynx was smallest and least compliant at the level of the velopharynx is consistent with a previous CT-based study (39). Although the 1.25-Hz rotation rate of the *a*OCT system is comparable with the acquisition rates of most CT and MRI scanners, it is not sufficient to track changes in airway caliber when breathing rates are rapid. This can be allowed for by synchronizing the *a*OCT images with other respiratory data, such as flow or volume change, and multiplexing images obtained over several breaths, so that the composite image is obtained relative to a particular phase of respiration. The need to do this would be obviated by increasing the rotation rate by at least a factor of three, which is an intended technological development.

A limitation of the technique is its capacity to view the complete circumference of the airway at all sites in all individuals. In some individuals, on some occasions, the probe may be positioned adjacent to an airway wall that is sufficiently concave or irregular to obscure parts of the airway wall from the probe's light beam. An example of this is the hypopharyngeal region (*see* Figures 2 and 3), in which the epiglottis can shadow the lower part of the retroglossal pharyngeal wall. In our experience, partial airway profiles occur most commonly at this level, but rarely in the velopharynx, where such gross irregularity of the airway is uncommon (*see* Figures 2 and 3). Where obscuration does limit measurement of parameters such as total pharyngeal area at that specific site, other useful parameters such as lateral extent of the airway are usually available.

Depending on the particular airway and location of the catheter, the scan range required to fully capture the airway cross-section could exceed a 26-mm radius (i.e., 52 mm total cross-section width), the current limit for our system. This is not a major limitation because individuals with OSA typically have either smaller pharynxes overall or a segment of the pharynx, which is narrower than average (16, 23). Nevertheless, it is possible to modify the instrument to extend the range in the future.

A challenge to imaging dimensions of the airway using *a*OCT is that there is longitudinal motion of the airway walls. It is possible, therefore, that the actual level of the structures that a fixed probe is measuring may vary over time as the airway structure moves in a ventrocaudal direction. Such movement was recently demonstrated by Liao and colleagues (40), who used cephalometry to document pharyngeal motion during a Mueller

maneuver in a group of patients with sleep-disordered breathing. They showed that, relative to measurements made at end-expiration, a Mueller maneuver increased the length of the pharyngeal airway by 2% in patients with mild OSA and by 6% in patients with moderate to severe OSA. The longitudinal and transmural forces generated during a wakeful Mueller maneuver most likely represent an extreme load on the upper airway, out of proportion to those produced by tidal breathing or by an obstructive event during sleep. Nevertheless, the effect of such longitudinal motion of the airway walls on *a*OCT-derived measurements of pharyngeal shape and size will need to be considered, perhaps by relating measurements to anatomical landmarks (such as the epiglottis tip).

Future Applications

Applied to clinical and research investigations of OSA, *a*OCT may allow determination of sites of and anatomic predispositions to airway collapse, the length of the collapsing regions and the relationship of collapse to transmural pressure gradients, phase of respiration, and state of sleep without restrictions on time or repetition. The capacity of *a*OCT to measure pharyngeal size and shape dynamically and repeatedly over extended periods at the bedside during sleep and wakefulness may provide useful additional information to aid OSA diagnosis and allow treatment to be devised on the basis of individual airway characteristics.

Conflict of Interest Statement: None of the authors have a financial relationship with a commercial entity that has an interest in the subject of this manuscript.

Acknowledgment: The authors thank the following individuals for their support and contributions to this work: Kathleen Maddison and Kelly Shepherd from the Department of Pulmonary Physiology, Sir Charles Gairdner Hospital; Peter Muir, Neil Hicks, and Associate Professor Vincent Low from the Department of Radiology, Sir Charles Gairdner Hospital; Alexandre Paduch, Stefan Schwer, and Jonathan Ng from the School of Electrical, Electronic and Computer Engineering, University of Western Australia.

References

1. Leiter J. Upper airway shape: is it important in the pathogenesis of obstructive sleep apnea? *Am J Respir Crit Care Med* 1996;153:894-898.
2. Rama AN, Tekwani SH, Kushida CA. Sites of obstruction in obstructive sleep apnea. *Chest* 2002;122:1139-1147.
3. Badr MS, Toiber F, Skatrud JB, Dempsey J. Pharyngeal narrowing occlusion during central sleep-apnea. *J Appl Physiol* 1995;78:1806-1815.

4. Hoffstein V, Fredberg JJ. The acoustic reflection technique for noninvasive assessment of upper airway area. *Eur Respir J* 1991;4:602–611.
5. Huang D, Swanson EA, Lin CP, Schuman JS, Stinson WG, Chang W, Hee MR, Flotte T, Gregory K, Puliafito CA, et al. Optical coherence tomography. *Science* 1991;254:1178–1181.
6. Drexler W, Morgner U, Ghanta RK, Kärtner FX, Schuman JS, Fujimoto JG. Ultrahigh-resolution ophthalmic optical coherence tomography. *Nat Med* 2001;7:502–507.
7. Bechara FG, Gambichler T, Stucker M, Orlikov A, Rotterdam S, Altmeyer P, Hoffmann K. Histomorphologic correlation with routine histology and optical coherence tomography. *Skin Res Technol* 2004;10:169–173.
8. Fujimoto JG, Boppart SA, Tearney GJ, Bouma BE, Pitris C, Brezinski ME. High resolution in vivo intra-arterial imaging with optical coherence tomography. *Heart* 1999;82:128–133.
9. Pitris C, Jesser C, Boppart SA, Stamper D, Brezinski ME, Fujimoto JG. Feasibility of optical coherence tomography for high-resolution imaging of human gastrointestinal tract malignancies. *J Gastroenterol* 2000;35:87–92.
10. Pan Y, Lavelle JP, Bastacky SI, Meyers S, Pirtskhalaishvili G, Zeidel ML, Farkas DL. Detection of tumorigenesis in rat bladders with optical coherence tomography. *Med Phys* 2001;28:2432–2440.
11. Bouma BE, Tearney GJ. Handbook of optical coherence tomography. New York: Marcel Dekker; 2002.
12. Armstrong JJ, Leigh MS, Walton ID, Zvyagin AV, Alexandrov SA, Schwer S, Sampson DD, Hillman DR, Eastwood PR. In vivo size and shape measurement of the human upper airway using endoscopic long-range optical coherence tomography. *Opt Express* 2003;11:1817–1826.
13. Polysomnography Task Force of the American Sleep Disorders Association Standards of Practice Committee. Practice parameters for the indications for polysomnography and related procedures. *Sleep* 1997;20:406–422.
14. Bland JM, Altman DG. Statistical methods for assessing agreement between two methods of clinical measurement. *Lancet* 1986;1:307–310.
15. Bland JM, Altman DG. Measurement error and correlation coefficients. *BMJ* 1996;313:41–42.
16. Haponik EF, Smith PL, Bohlman ME, Allen RP, Goldman SM, Bleecker ER. Computerized tomography in obstructive sleep apnea: correlation of airway size with physiology during sleep and wakefulness. *Am Rev Respir Dis* 1983;127:221–226.
17. Shepard JW Jr, Stanson AW, Sheedy PF, Westbrook PR. Fast-CT evaluation of the upper airway during wakefulness in patients with obstructive sleep apnea. *Prog Clin Biol Res* 1990;345:273–282.
18. Lowe AA, Fleetham JA, Adachi S, Ryan CF. Cephalometric and computed tomographic predictors of obstructive sleep apnea severity. *Am J Orthod Dentofacial Orthop* 1995;107:589–595.
19. Tsushima Y, Antila J, Svedstrom E, Vetrio A, Laurikainen E, Polo O, Kormano M. Upper airway size and collapsibility in snorers: evaluation with digital fluoroscopy. *Eur Respir J* 1996;9:1611–1618.
20. Wheatley JR, Kelly WT, Tully A, Engel LA. Pressure-diameter relationships of the upper airway in awake supine subjects. *J Appl Physiol* 1991;70:2242–2251.
21. Arens R, Sin S, McDonough JM, Palmer JM, Dominguez T, Meyer H, Wootton DM, Pack AI. Changes in upper airway size during tidal breathing in children with obstructive sleep apnea syndrome. *Am J Respir Crit Care Med* 2005;171:1298–1304.
22. Schwab RJ, Pasirstein M, Pierson R, Mackley A, Hachadoorian R, Arens R, Maislin G, Pack AI. Identification of upper airway anatomic risk factors for obstructive sleep apnea with volumetric magnetic resonance imaging. *Am J Respir Crit Care Med* 2003;168:522–530.
23. Schwab RJ, Gupta KB, Gefter WB, Metzger LJ, Hoffman EA, Pack AI. Upper airway and soft tissue anatomy in normal subjects and patients with sleep-disordered breathing: significance of the lateral pharyngeal walls. *Am J Respir Crit Care Med* 1995;152:1673–1689.
24. Donnelly LF, Surdulescu V, Chini BA, Casper KA, Poe SA, Amin RS. Upper airway motion depicted at cine MR imaging performed during sleep: comparison between young patients with and those without obstructive sleep apnea. *Radiology* 2003;227:239–245.
25. Isono S, Morrison DL, Launois SH, Feroah TR, Whitelaw WA, Remmers JE. Static mechanics of the velopharynx of patients with obstructive sleep apnea. *J Appl Physiol* 1993;75:148–154.
26. Rowley JA, Sanders CS, Zahn BR, Badr MS. Effect of REM sleep on retroglossal cross-sectional area and compliance in normal subjects. *J Appl Physiol* 2001;91:239–248.
27. Guilleminault C, Hill MH, Simmons FB, Powell N, Riley R, Stoohs R. Passive constriction of the upper airway during central apneas: fiberoptic and EMG investigations. *Respir Physiol* 1997;108:11–22.
28. Morrell MJ, Badr MS. Effects of NREM sleep on dynamic within-breath changes in upper airway patency in humans. *J Appl Physiol* 1998;84:190–199.
29. Mohsenin V. Gender differences in the expression of sleep-disordered breathing: role of upper airway dimensions. *Chest* 2001;120:1442–1447.
30. Kamal I. Acoustic pharyngometry patterns of snoring and obstructive sleep apnea patients. *Otolaryngol Head Neck Surg* 2004;130:58–66.
31. Taskforce. Sleep-related breathing disorders in adults: recommendations for syndrome definition and measurement techniques in clinical research: the Report of an American Academy of Sleep Medicine Task Force. *Sleep* 1999;22:667–689.
32. Oeverland B, Akre H, Kvaerner KJ, Skatvedt O. Patient discomfort in polysomnography with esophageal pressure measurements. *Eur Arch Otorhinolaryngol* 2005;262:241–245.
33. Skatvedt O, Akre H, Godtlibsen OB. Nocturnal polysomnography with and without continuous pharyngeal and esophageal pressure measurements. *Sleep* 1996;19:485–490.
34. Chervin RD, Aldrich MS. Effects of esophageal pressure monitoring on sleep architecture. *Am J Respir Crit Care Med* 1997;156:881–885.
35. Hessel NS, Laman M, van Ammers VC, van Duijn H, de Vries N. Feasibility study of Flextube reflectometry for localisation of upper airway obstruction in obstructive sleep apnea. *Rhinology* 2003;41:87–90.
36. Sanders MH, Rogers RM, Pennock BE. Prolonged expiratory phase in sleep apnea: a unifying hypothesis. *Am Rev Respir Dis* 1985;131:401–408.
37. Morrell MJ, Arabi Y, Zahn B, Badr MS. Progressive retropalatal narrowing preceding obstructive apnea. *Am J Respir Crit Care Med* 1998;158:1974–1981.
38. Schwab RJ, Gefter WB, Hoffman EA, Gupta KB, Pack AI. Dynamic upper airway imaging during awake respiration in normal subjects and patients with sleep disordered breathing. *Am Rev Respir Dis* 1993;148:1385–1400.
39. Kuna ST, Bedi DG, Ryckman C. Effect of nasal airway pressure on upper airway size and configuration. *Am Rev Respir Dis* 1988;138:969–975.
40. Liao YF, Huang CS, Chuang ML. The utility of cephalometry with the Muller maneuver in evaluating the upper airway and its surrounding structures in Chinese patients with sleep-disordered breathing. *Laryngoscope* 2003;113:614–619.